Inorganica Chimica Acta 428 (2015) 51–56

Contents lists available at ScienceDirect

Inorganica Chimica Acta

journal homepage: www.elsevier.com/locate/ica

Silver nitroprusside: Atypical coordination within the metal nitroprussides series

J. Rodríguez-Hernández [a,b], L. Reguera [c], A.A. Lemus-Santana [d], E. Reguera [d,*]

[a] Instituto de Ciencia y Tecnología de Materiales, Universidad de La Habana, Cuba
[b] Instituto de Investigaciones en Materiales, Universidad Nacional Autónoma de México, Mexico
[c] Facultad de Química, Universidad de La Habana, Cuba
[d] Centro de Investigación en Ciencia Aplicada y Tecnología Avanzada, Unidad Legaria, Instituto Politécnico Nacional, Mexico

ARTICLE INFO

Article history:
Received 7 October 2014
Received in revised form 18 December 2014
Accepted 18 December 2014
Available online 30 January 2015

Keywords:
Nitroprusside
Coordination polymer
Crystal structure
Cyanide bridge
Silver compound

ABSTRACT

The nitroprusside complex anion forms an insoluble salt, of formula unit $Ag_2[Fe(CN)_5NO]$, when it reacts with an aqueous solution of Ag^+. Related to the high insolubility of silver halides, silver nitroprusside is a good intermediate to obtain soluble nitroprussides of alkaline, alkaline earth and trivalent transition metals. No other applications for that solid have been reported, probably because its crystal structure and related properties are unknown. This contribution reports the crystal structure for the titled compound from X-ray powder diffraction data and its refinement using the Rietveld method. It crystallizes with a monoclinic unit cell, in the *Pc* space group, with cell parameters: $a = 7.4254(3)$, $b = 6.4121(2)$, $c = 11.8729(2)$ Å, $\beta = 115.16(1)°$. The crystal structure has two sites for the silver atom, corresponding to its coordination two and three to the N ends of CN groups. Calculation of the radial distribution function and IR and UV–Vis spectra provided the *a priori* structural information required to support the selected structural model to be refined. Such information was then used to validate the refined structure. The structure of this compound is atypical within the metal nitroprussides series. The thermal decomposition in air and nitrogen atmosphere of the title compound was studied from thermogravimetry and IR combined techniques. In the solid residues metallic silver and iron oxide (hematite) were identified.

1. Introduction

The existence of the pentacyanonitrosylferrate complex anion, $[Fe(CN)_5NO]^{2-}$, commonly known as nitroprusside, and its salts were first reported by Plaifair in 1848 [1]. During the following hundred years practically all the published works dealt on its soluble salts, particularly, on sodium nitroprusside, related to its optical properties and medical applications [2]. The preparation and characterization of the insoluble salts are documented from 1950s years [3–9]. The nitroprusside complex anion forms insoluble solids with monovalent and divalent transition metals. For Mn^{2+}, Fe^{2+}, Co^{2+}, Ni^{2+}, Cu^{2+}, Zn^{2+} and Cd^{2+} their crystal structures have been reported from X-ray diffraction data using single crystals grown by slow diffusion techniques [10–14]. Except for Co and Ni, the formed solid crystallizes with different unit cell and space group, depending on the preparative route used and on the amount of water molecules per formula unit found in the structure [15]. That series of coordination compounds has an open framework 3D structure with pore size appropriate for the storage and separation of small molecules, among them H_2, O_2, N_2, CO_2, H_2O and CH_4 [16–20]. The nitroprusside anion also forms insoluble salts also with Ag^+, Hg^+, Hg^{2+} and Cu^+, but except for Hg^+ [21], their crystal structure and related properties are unknown.

Sodium nitroprusside is the commercial available source for the nitroprusside complex anion. When the soluble salt of other metals is required, e.g. alkaline earth metals, trivalent transition metals, and post-transition metals, the synthetic route involves the preparation of silver nitroprusside as an intermediate, to finally obtain the desirable metal nitroprusside by adding a solution of the metal chloride onto powder of silver nitroprusside. Alkaline and alkaline earth nitroprussides have received large attention because of their optical properties as holographic memory materials [22]. Except that use as intermediate in the synthesis of other metal nitroprussides, no other potential application for the titled compound have been reported, probably by the fact that its crystal structure and related properties are unknown.

The structural chemistry of the nitroprusside anion is well documented and also the mechanism of interaction with metal species [23]. This anion forms coordination bonds with transition metals

* Corresponding author.
E-mail address: edilso.reguera@gmail.com (E. Reguera).

http://dx.doi.org/10.1016/j.ica.2014.12.023
0020-1693/

through the N end of the CN groups while the O end on the NO group remains unlinked.

This contribution reports the crystal structure for silver nitroprusside, solved from XRD powder patterns using calculation of the radial distribution function (RDF) combined with global optimization in the direct space (simulated annealing). The derived model was then refined by the Rietveld method. The recorded IR, UV–Vis spectra and thermogravimetric (TG) data provided *a priori* structural information to select the appropriate structural model. That information is then used to validate the results of its refinement. The material behavior on heating in air and nitrogen atmosphere was studied from thermogravimetric analysis and recording the IR spectra of the evolved gases. The phases present in the solid residues were identified from XRD and IR data.

2. Experimental

The titled compound was prepared by the precipitation method from aqueous solutions (0.01 M) of silver nitrate and sodium nitroprusside, both from Sigma–Aldrich. The formed precipitate was aged within the mother liqueur for a week in the darkness and then separated by centrifugation and washed several times with distilled water. The obtained pasty solid was dried in air in the darkness until it has constant weight. The nature of resulting fine powder as $Ag_2[Fe(CN)_5NO]$ was established from X-ray energy-dispersed (EDS) and IR spectroscopies. According to EDS spectra, the Ag:Fe atomic ratio in the solid is 2:1, while the recorded IR spectrum is typical of metal nitroprussides. The recording of the thermogravimetric (TG) curve, X-ray powder pattern, and UV–Vis spectrum completed the material characterization. The material decomposition on heating, in both nitrogen and air atmosphere, was monitored by combined TG and IR techniques.

IR spectrum was recorded with a Pike ATR device using a Perkin spectrophotometer. UV–Vis spectrum was collected with the integration sphere method. The TG curve was recorded both in air and under an N_2 flow (1 L/min) using a TA Instrument (IR-5000) operated in the HR mode. The XRD powder patterns were collected in Bragg–Brentano geometry at room temperature with both Cu Kα and Mo Kα radiation. The patterns recorded with this last radiation was used to calculate the radial distribution function (RDF) in order to obtain *a priori* information on the interatomic distances involving heavy atoms. The unit cell was previously identified and its parameters calculated during the Miller indexes assignment with the help of TREOR and DICVOL algorithms [24]. The interatomic distances obtained from the RDF calculation were used to discriminate between all the possible space groups to be considered in the structural refinement. The structural model was finally identified using a global optimization process in the direct space (*simulated annealing*) implemented in the EXPO09 program [25]. The crystal structure was refined using the Rietveld method with the FULLPROF program [26]. Details on the XRD data recording and processing are available from Supplementary information.

As already mentioned, transition metal nitroprussides have received certain attention as prototype of porous solids for hydrogen storage [19,20], and in that sense, H_2 adsorption isotherms were recorded at 75 K in order to explore a possible hydrogen molecule interaction with the silver atom in the structure of silver nitroprusside.

3. Results and discussion

3.1. IR and UV–Vis spectra of silver nitroprusside

Silver nitroprusside is obtained as fine pink color powder. Fig. 1 shows its IR spectrum. The spectral region of ν(OH) vibrations is free of absorption bands, which suggests that this compound is anhydrous. Such evidence is supported by the recorded TG curve (discussed below). No weight loss on heating below 160 °C was detected. Metal nitroprussides usually dehydrate below 120 °C [17–19]. From this fact, the narrow IR absorption band that is observed at 3856 cm^{-1} was assigned to an overtone of the NO stretching vibration, which is observed at 1934 cm^{-1}. The frequency difference of this overtone relative to $2\nu_{NO}$ is 12 cm^{-1}, which was ascribed to an anharmonicity effect. The ν(CN) vibration appears as two absorption bands separated 14 cm^{-1}, at 2176 and 2162 cm^{-1} which were ascribed, according to their intensities ratio, to equatorial and axial CN groups, respectively. The lower frequency for the axial CN group suggests that it remains unlinked or its bond to the silver atom is relatively weak, at least compared with the one corresponding to the equatorial ligands. An analog CN stretching bands configuration, but with a greater frequency difference (47 cm^{-1}) is observed for the orthorhombic phase of copper (II) nitroprusside where the equatorial CN groups are found linked to copper atoms but the axial one remains unlinked [27]. For the tetragonal phase of copper nitroprusside, where the axial CN group is found coordinated to a copper atom, the vibration for the equatorial and axial CN groups are observed at 2208 and 2196 cm^{-1}, respectively, for a frequency difference of 12 cm^{-1}, similar to the value observed for silver nitroprusside. This suggests that in the compound under study, the axial CN group remains linked to a silver atom. The possible axial CN group coordination to a silver atom is also inferred from the frequency value for ν(NO) vibration, which is observed in 1934 cm^{-1}. In sodium nitroprusside this vibration is observed at 1938 cm^{-1} (see Supplementary information). For the orthorhombic and tetragonal phases of copper nitroprussides, that vibration is found at 1957 and 1949 cm^{-1}, respectively. The frequency shift of 8 cm^{-1}, for the stretching of the NO group results from an induced effect by also the coordination of the axial CN group a copper atom. Below 1000 cm^{-1} five well-resolved absorption bands appear (Fig. 1, Inset), at 661, 648, 519, 446 and 432 cm^{-1}. According to reported studies on IR and Raman spectra of metal nitroprussides [28], these bands were ascribed to δ(FeNO), ν(FeN), $\delta(FeCN)_{eq.+ax}$, $\nu(FeC)_{eq,\ A'+A''}$ and $\nu(FeC)_{eq,\ A'}$ vibrations, respectively. These vibrations show slight frequency shift relative to the values found for the sodium nitroprusside precursor salt, which is sensing changes in the electronic structure of the complex anion on the coordination bond formation.

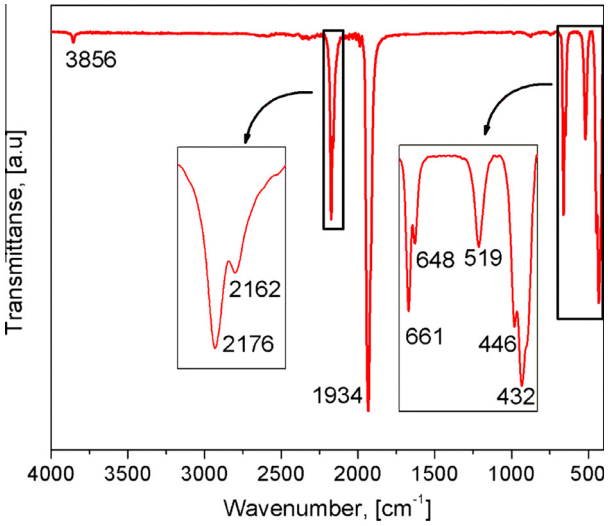

Fig. 1. IR spectrum of silver nitroprusside, $Ag_2[Fe(CN)_5NO]$.

UV–Vis spectrum for the obtained powder is typical of a metal nitroprusside (see Supplementary information). The observed

bands at 256, 396 and 500 nm, were ascribed to 11e → 13e, 12e → 13e, and $2b_2$ → 13e metal–ligand electronic transitions, respectively [29]. The broadening for the band at 256 nm is probably related to certain contribution from the 12e → $4b_1$ transition. Because the silver ion has a $4d^{10}$ electronic configuration, no d–d transitions are observed in the UV–Vis spectrum.

3.2. Crystal structure

Fig. 2 shows the recorded XRD powder pattern for silver nitroprusside. This compound crystallizes with a monoclinic unit cell in the *Pc* space group and cell parameters: $a = 7.4254(3)$, $b = 6.4121(2)$, $c = 11.8729(2)$ Å, and $\beta = 115.16(1)°$. The unit cell accommodates two formula units ($Z = 2$). Fig. 2 (Inset) shows the RDF calculated from the XRD powder pattern recorded with Mo Kα radiation (Table 1). The intense peaks observed at 3.20 and 5.17 Å correspond to Ag–Ag and Fe–Ag interatomic distances, respectively. The assignment for the peak found at 5.17 Å as related to Fe–Ag distance is supported by the Fe–CN–T chain length observed in metal nitroprussides [10–14,27,28]. The electron density of the involved atoms determines the peak intensity in RDF, and from this fact the 3.20 Å peak was assigned to Ag–Ag interatomic distance.

From the recorded XRD powder pattern, four possible space group were identified (*P2*, *Pm*, *P2/m* and *Pn*). According to direct methods implemented in EXPO09 program [25], only *P2* and *Pn* space groups lead to solution with Ag–Ag and Fe–Ag interatomic distances (Ag–Ag = 3.18 Å, Fe–Ag = 5.20 Å), congruent with the values found from the RDF calculation. The Fourier synthesis discarded the *P2* space group. The appropriate structural model was finally found within the *Pn* space group using a global optimization procedure in the direct space (*simulated annealing*) from an initially proposed asymmetric cell. Because this is a non-standard symmetry group, an axes transformation leads to the standard *Pc* group, which was the model to be refined. Fig. 2 shows that this model produces an excellent fitting for the experimental XRD pattern. Fig. 3 shows the coordination environment for the involved metals. Two types of silver atoms were found; Ag1 with linear coordination to cyanide ligands at their N ends, and Ag_2 coordinated to three CN groups. As expected, the iron atom is coordinated to five CN groups at the C ends and to the N end of the NO ligand. Similar to the reported for other members of the metal nitroprussides series, the NO group remains unlinked at its O end [10–14,27]. In the solid, the five CN groups were found linked to silver atoms. In the equatorial plane, the silver atoms have a linear coordination with CN group, through a relatively strong bond, $\langle Ag–N_{CNeq}\rangle = 2.077$ Å,

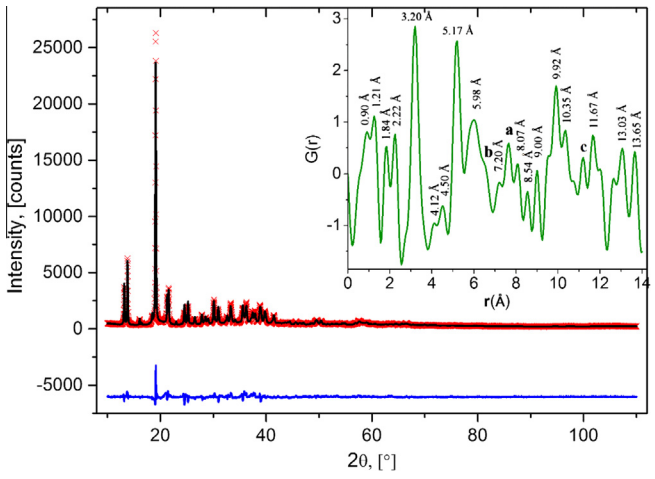

Fig. 2. XRD powder pattern for silver nitroprusside and its fitting from the Rietveld refinement. Inset: Calculated radial distribution function from an XRD pattern recorded with Mo Kα radiation.

Table 1
Assignment of relevant maxima in the calculated FRD function.

Interatomic distances (Å)	Assignment
1.21	C≡N/N═O
1.84	Fe—C
2.22	Ag—N
3.20	Ag—Ag
5.17	Fe—Ag
6.51	*b*
7.57	*a*
11.67	*c*

to form a system of undulated layers. The axial CN group is linked to Ag_2 atom ($Ag_2–N_{CNax} = 2.392$ Å). The silver atoms coordinated to the equatorial CN groups are found at 2.856 Å from the axial NO group, which discards the possibility of silver atom coordination to the axial NO group. Neighboring $(Ag_2[Fe(CN)_5NO])_n$ chains remain linked through Ag2–N_{CNax} coordination. The refined structural model for silver nitroprusside is supported by the above discussed IR spectra.

The relatively weak bond of the axial CN group at its N end to a silver atom from a neighboring layer is supported by the recorded IR spectrum (Fig. 1). The CN stretching frequency of that bridge axial ligand is found only 14 cm^{-1} below the frequency corresponding to the equatorial ones. A linear coordination for the silver atom has been reported for silver hexacyanides, which are materials with colossal negative thermal expansion [30]. From this fact, an analog behavior is expected for silver nitroprusside. For divalent transition metal nitroprussides, negative thermal expansion have also been reported [31].

Table 2 summarizes the refined atomic positions. Table 3 contains the calculated interatomic distances and angles. These interatomic distances are within the expected range for transition metal nitroprussides [10–14,21,27,28]. The calculated Ag–Ag distance, 3.18 Å, is quite similar to the value found from RDF calculation (3.20 Å). The C–Fe–C angles are close to 90°, as expected for a pseudo-octahedral coordination. The equatorial Fe–C–N angle deviates from the linearity related to the ligand coordination also to the silver atom. This angle is in average 176.05°. Structural information derived from the crystal structure refinement has been deposited at ICSD database.

The crystal structure of nitroprussides of monovalent Group 1 ion was extensively studied about three decades ago [32–34]. The nitroprusside anion forms soluble salts with these metals and also with alkali earth ones [35], where the interaction between the nitroprusside anion with the metal is of electrostatic nature. In silver nitroprusside the silver atom forms a relatively strong coordination bond with the N ends of the nitroprusside anion, similar to the observed for the 3d metals [10–14].

3.3. Material behavior on heating

The behavior of metal nitroprussides on heating is well documented [36,37]. The thermal decomposition of a solid is related to the rupture of chemical bonds as consequence of an increasing amplitude for the vibrations of atoms around their equilibrium positions due to the increase of the thermal energy (kT). From this fact, for metal nitroprussides the unbridged NO ligand evolves at relatively low temperature, usually below 200 °C, and also the axial CN group if it remains unbridged or weakly bonded to a metal center. The unbridged ligands are particularly susceptible to evolve on heating. The loss of the NO ligand leads to formation of intermediate metal cyanide complexes of diverse stoichiometry, depending of the involved metals [34,37]. On progressive heating, the formed metal cyanides decompose with evolution of cyanide ligands. The

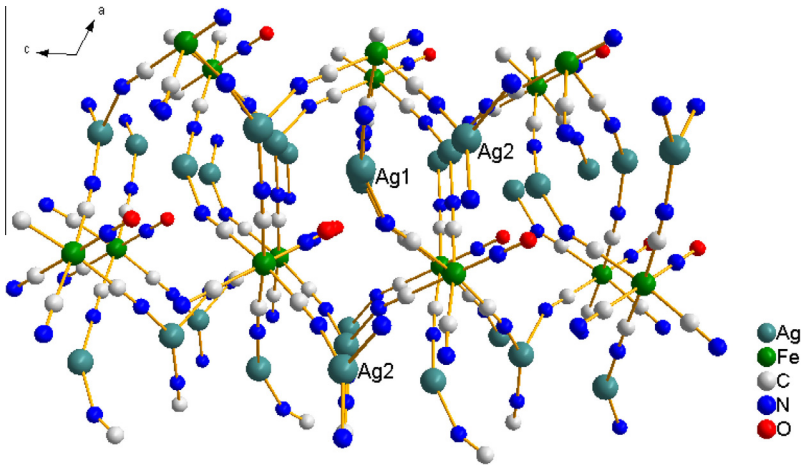

Fig. 3. Framework of silver nitroprusside and coordination environments for the involved metals (Fe and Ag). In the structure, there are two types silver atoms (Ag1 and Ag2) at a distance of 3.165(3) Å. The NO group remains unlinked at its O end.

Table 2
Atomic positions and temperature and occupation factors derived from the Rietveld refined crystal structure for $Ag_2[Fe(CN)_5NO]$.

Atom	Site	X	Y	Z	Biso	Occ
Fe	2a	0.893(2)	0.488(2)	0.811(2)	1.34(2)	1
Ag1	2a	0.337(2)	−0.061(2)	0.686(2)	2.45(2)	1
Ag2	2a	0.486(2)	1.004(2)	0.477(2)	2.81(3)	1
C1	2a	0.673(4)	0.298(5)	0.769(3)	3.94(3)	1
N1	2a	0.547(4)	0.178(5)	0.740(3)	3.94(3)	1
C2	2a	0.772(4)	0.647(6)	0.897(4)	3.94(3)	1
N2	2a	0.699(4)	0.742(6)	0.949(4)	3.94(3)	1
C3	2a	1.097(5)	0.700(6)	0.864(4)	3.94(3)	1
N3	2a	1.226(5)	0.817(6)	0.899(4)	3.94(3)	1
C4	2a	0.736(4)	0.655(5)	0.667(4)	3.94(3)	1
N4	2a	0.643(4)	0.764(5)	0.586(4)	3.94(3)	1
C5	2a	1.034(6)	0.342(4)	0.966(4)	3.94(3)	1
N5	2a	1.110(6)	0.247(4)	1.056(4)	3.94(3)	1
N6	2a	0.998(4)	0.351(4)	0.736(4)	3.94(3)	1
O1	2a	1.069(4)	0.258(4)	0.685(4)	3.94(3)	1

Table 3
Calculated inter-atomic distances (in Å) and bond angles (in °) from the refined structure for $Ag_2[Fe(CN)_5NO]$.

Bond distance (Å)	Bond angles (°)	
Fe–C1 = 1.928(3)	C1–Fe–C2 = 86.1(3)	N1–Ag1–N5 = 154.5(4)
Fe–C2 = 1.929(5)	C1–Fe–C3 = 172.1(3)	N3–Ag2–N4 = 150.3(3)
Fe–C3 = 1.928(4)	C1–Fe–C4 = 89.7(3)	N2–Ag2–N3 = 96.1(2)
Fe–C4 = 1.929(4)	C1–Fe–C5 = 89.7(2)	N2–Ag2–N4 = 111.7(3)
Fe–C5 = 1.928(4)	C1–Fe–N6 = 93.9(3)	Fe–C1–N1 = 176.0(4)
Fe–N6 = 1.659(5)	C2–Fe–C3 = 86.0(3)	Fe–C2–N2 = 179.9(5)
Ag1–N1 = 2.081(3)	C2–Fe–C4 = 86.1(3)	Fe–C3–N3 = 176.0(4)
Ag1–N5 = 2.108(4)	C2–Fe–C5 = 86.1(3)	Fe–C4–N4 = 176.1(4)
Ag2–N3 = 2.089(4)	C2–Fe–N6 = 179.9(5)	Fe–C5–N5 = 176.1(4)
Ag2–N4 = 2.033(3)	C3–Fe–C4 = 89.7(2)	Fe–N6–O1 = 179.9(5)
Ag2–N2 = 2.392(4)	C3–Fe–C5 = 89.7(3)	Ag1–N1–C1 = 174.0(3)
C1–N1 = 1.149(4)	C3–Fe–N6 = 93.9(3)	Ag1–N5–C5 = 155.0(4)
C2–N2 = 1.148(6)	C4–Fe–C5 = 172.2(3)	Ag2–N3–C3 = 172.0(4)
C3–N3 = 1.149(5)	C4–Fe–N6 = 93.9(4)	Ag2–N4–C4 = 166.4(4)
C4–N4 = 1.149(5)	C5–Fe–N6 = 93.9(4)	Ag2–N2–C2 = 157.3(5)
C5–N5 = 1.149(5)		
N6–O1 = 1.123(6)		

Ag1–Ag2 = 3.165(3) Å; Ag1–Ag1 = 6.412(1) Å; Ag2–Ag2 = 6.412(1) Å.

evolved cyanide radicals have reducing character resulting the formation of C_2N_2 and reduced species of the involved metals [38].

Fig. 4 shows the recorded TG curve in a nitrogen atmosphere for silver nitroprusside. According to the derivative of that curve, the thermal decomposition of the solid under study occurs in four steeps. The first thermal effect is observed from 150 °C with a maximum decomposition rate close to 200 °C. The weight loss for this effect is 13% and is ascribed to the evolution of the unbridged NO ligand and to the weakly bonded axial CN group. The second weight loss has a maximum at 250 °C and it was assigned to decomposition of an intermediate metal cyanide of low thermal stability. Then, from 280 °C a pronounced weight loss takes place, which has a maximum at 325 °C. This effect is also ascribed to decomposition of intermediate cyanide metals. The fourth effect is detected from 350 °C as a slight inflection in the TG curve. It seems, the decomposition of the final intermediate cyanide has a low kinetic and a relatively high thermal stability. In a non-oxidant atmosphere, under a nitrogen flow for instance, the expected final products of the thermal decomposition of metal cyanides are the involved metals in metallic state related to the reducing effect of the cyanide radicals [38]. Fig. 4 (Inset) shows the sequence of IR spectra corresponding to the evolved gases during the thermal decomposition process. For all the temperature range an intense doublet close to 2300 cm^{-1} is observed, which correspond to cyanogen (C_2N_2) species [39]. The IR spectra profile has four maxima which could be related to the four inflections observed in the recorded TG curve, corresponding to the already mentioned solid decomposition through four thermal effects. The release of the NO group is detected as relatively weak signal in the 1827–1734 cm^{-1} spectral region due to presence of nitrogen monoxide species (see Supplementary information). An analog behavior is observed for the solid decomposition under an air atmosphere. In the TG curve four thermal effects are clearly identified while the IR spectra of the evolved gases are dominated by the cyanogen doublet (see Supplementary information).

According to XRD data (see Supplementary information), the solid residue for both, the samples heated under a nitrogen atmosphere and in air, is formed by metallic silver and iron oxide (hematite). The presence of Fe_2O_3 as final iron phase under a nitrogen atmosphere, suggests that metallic iron is formed by the reducing effect of the evolved cyanide radicals, which is then oxidized when the residue is exposed to air. Such behavior has been observed for the thermal decomposition of Prussian blue under nitrogen and in vacuum [38]. No signals from cyanide metal complexes were found in the residues (see Supplementary information).

3.4. Hydrogen adsorption

The hydrogen molecule forms lateral coordination compounds with transition metals of low valence and extended t_{2g} orbitals

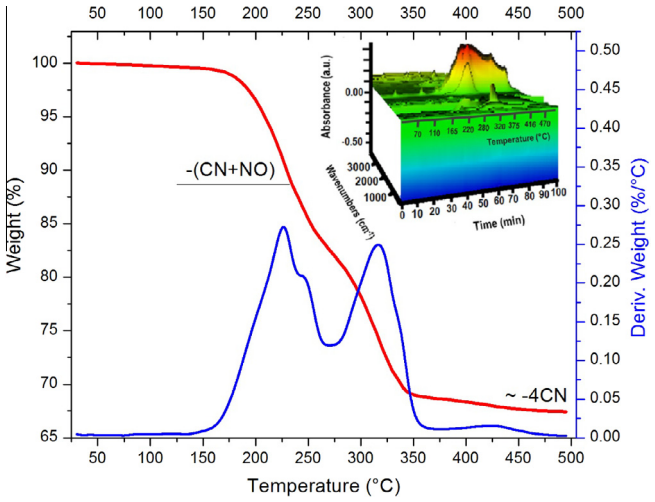

Fig. 4. TG curve recorded under a nitrogen atmosphere and its derivative for silver nitroprusside. Inset: Normalized IR spectra of the evolved gases on the sample heating.

[40]. In this sense, H_2 coordination to available coordination sites in complexes of osmium, molybdenum, tungsten, copper, titanium and vanadium ions have been reported [40–43]. As discussed above, the silver atom in the compound under study has available coordination sites to accept the coordination of hydrogen molecules; however, to the best of our knowledge, such possibility in silver compound has not been explored. Fig. 5 shows the recorded H_2 adsorption isotherm at 75 K in $Ag_2[Fe(CN)_5NO]$. This figure also includes the adsorption isotherm for the Ni analogue. This last solid has a relative high H_2 uptake ability, attributable to the presence of certain contribution of coordination type interaction to the sorption forces [20]. For the silver compound, the amount of H_2 adsorbed is quite low and the isotherm shows a practically linear dependence on the absolute pressure. Such behavior has two possible causes, inaccessibility of the material porous framework to the hydrogen molecule or a weak adsorbate interaction with the cavity surface. The formation of a coordination bond involves a relatively high sorption energy and the isotherm must saturate at relatively low pressure, with a high slope at low pressure values, which was not observed. The hydrogen molecule has a kinetic diameter of 2.9 Å [44]. The cavity diameter is close to the Ag1–Ag2 interatomic distance, which is 3.18 Å, according to the refined atomic positions. However, silver ion has an ionic radius of 0.67 Å [45], and the available windows size results 2.84 Å, below the kinetic diameter for the hydrogen molecule, 2.9 Å. This suggests that the porous framework of silver nitroprusside is inaccessible to the hydrogen molecule.

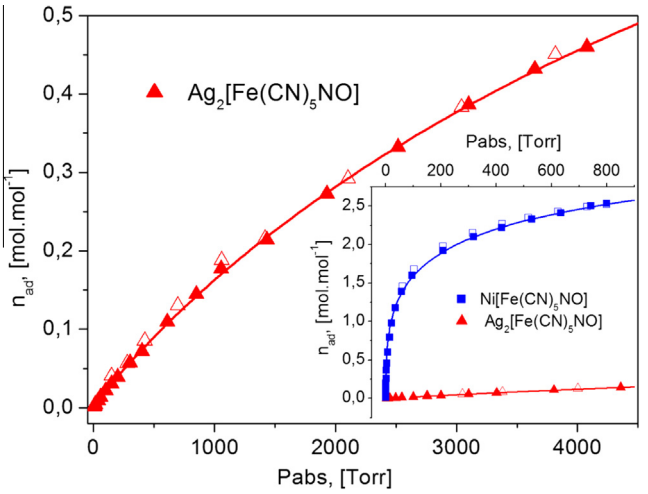

Fig. 5. Hydrogen adsorption isotherm at 75 K in silver nitroprusside. For comparison, the Inset also shows the H_2 adsorption isotherm in the Ni analogue.

4. Conclusions

Silver nitroprusside, $Ag_2[Fe(CN)_5NO]$, crystallizes with a monoclinic unit cell in the *Pc* space group. The unit cell contains two formula units of the compound. In the crystal structure, to types of silver atoms are found; Ag1 linearly coordinated to the N ends of the equatorial CN groups, and Ag2 also coordinated to the axial CN ligand, through a weaker interaction. This last coordination interaction supports the material 3D framework. The crystal structure of silver nitroprusside is atypical within metal nitroprusside series; with two types of coordination (2 and 3) for the metal linked at the N end of the CN group. The refined crystal structure is supported by the available spectroscopic information. On the solid heating, NO and the axial CN groups evolve from about 160 °C and then the thermal decomposition is completed by evolution of also the axial CN groups. In the solid residues metallic silver and iron oxides were identified. The studied solid was considered as a model to shed light on the possible coordination interaction between the silver atom and hydrogen molecules. However, the porous framework of silver nitroprusside results inaccessible to the hydrogen molecule.

Acknowledgements

This study was partially supported by the CONACYT – Mexico projects 2011-01-174247, FON.INST./75/2012 and 154626. The authors thank the help of Dr. A. Gómez from University of Guelph (Canada) for recording the XRD pattern for RDF calculation, and to Dr. E. Torres for the TG-IR combined data collection.

Appendix A. Supplementary material

Details on the XRD data recording and processing, and IR spectra of evolved gases during the solid heating in air and in N_2 atmosphere. Structural information derived from the crystal structure refinement has also been deposited at ICSD Fachinformationszentrum Karlsruhe (FIZ) (E-mail: crysdatafiz-karlsruhe.de) with CSD file number: 427798: $Ag_2[Fe(CN)_5NO]$. Supplementary data associated with this article can be found, in the online version, at http://dx.doi.org/10.1016/j.ica.2014.12.023.

References

[1] L. Playfair, Proc. R. Soc., Lond. 5 (1848) 846.
[2] A.R. Butler, I.L. Megson, Chem. Rev. 102 (2002) 1155.
[3] P.G. Salvadeo, Gazz. Chim. Ital. 89 (1959) 2184.
[4] L.A. Gentil, E.J. Baran, P.J. Aymonino, Z. Naturforsch. 23b (1968) 1264.
[5] J.B. Ayres, W.H. Waggoner, J. Inorg. Nucl. Chem. 31 (1969) 2045.
[6] A.N. Garg, P.S. Goel, Inorg. Chem. 10 (1971) 1344.
[7] H. Inoue, H. Iwase, S. Yanagisawa, Inorg. Chim. Acta 7 (1973) 259.
[8] D.B. Brown, Inorg. Chem. 14 (1975) 2582.
[9] L.A. Gentil, E.J. Baran, P.J. Aymonino, Inorg. Chim. Acta 20 (1976) 251.
[10] D.F. Mullica, D.B. Tippin, E.L. Sappenfield, D.H. Leschnitzer, Inorg. Chim. Acta 164 (1989) 99.
[11] D.F. Mullica, D.B. Tippin, E.L. Sappenfield, Inorg. Chim. Acta 174 (1990) 129.
[12] D.F. Mullica, D.B. Tippin, E.L. Sappenfield, J. Crystal. Spectrosc. Res. 21 (1991) 81.
[13] D.F. Mullica, D.B. Tippin, E.L. Sappenfield, J. Coord. Chem. 24 (1991) 83.
[14] D.F. Mullica, D.B. Tippin, E.L. Sappenfield, J. Coord. Chem. 25 (1992) 175.
[15] E. Reguera, A. Dago, A. Gómez, J.F. Bertrán, Polyhedron 15 (1996) 3139.
[16] G. Boxhoorn, J. Moolhuysen, J.G.F. Coolegen, R.A. van Santen, J. Chem. Soc., Chem. Commun. 1305 (1985).
[17] J. Balmaseda, E. Reguera, A. Gómez, J. Roque, C. Vázquez, M. Autie, J. Phys. Chem. B 107 (2003) 11360.

[18] J.T. Culp, C. Matranga, M. Smith, E.W. Bittner, B. Bockrath, J. Phys. Chem. B 110 (2006) 8325.
[19] L. Reguera, J. Balmaseda, C.P. Krap, E. Reguera, J. Phys. Chem. C 112 (2008) 10490.
[20] L. Reguera, J. Roque, J. Hernández, E. Reguera, Int. J. Hydrogen Energy 35 (2010) 12864.
[21] H. Osiry, A. Cano, L. Reguera, A.A. Lemus-Santana, E. Reguera, J. Solid State Chem. 221 (2015) 79.
[22] S. Haussühl, G. Schetter, Th. Woike, Opt. Commun. 114 (1995) 219.
[23] L.M. Baraldo, P. Forlano, A.R. Parise, L.D. Slep, J.A. Olabe, Coord. Chem. Rev. 219–221 (2001) 881. and references therein.
[24] D. Louer, R. Vargas, J. Appl. Crystallogr. 15 (1982) 542.
[25] A. Altomare, C. Cuocci, C. Giacovazzo, A. Moliterni, R. Rizzi, N. Corriero, A. Falcicchio, J. Appl. Crystallogr. 46 (2013) 1231.
[26] J. Rodríguez-Carvajal, The FullProf Program, Institute Leon Brillouin, Saclay, France, 2000.
[27] A. Gómez, J. Rodríguez-Hernández, E. Reguera, J. Chem. Crystallogr. 34 (2004) 893.
[28] A. Benavante, J.A. de Morán, O.E. Piro, E.E. Castellano, P.J. Aymonino, J. Chem. Crystallogr. 27 (1997) 343.
[29] P.T. Manoharan, H.B. Gray, J. Am. Chem. Soc. 87 (1965) 3340.
[30] A.L. Goodwin, M. Calleja, M.J. Conterio, M.T. Dove, J.S.O. Evans, D.A. Keen, L. Peters, M.G. Tucker, Science 319 (2008) 794.
[31] T. Matsuda, J. Kim, Y. Moritomo, RSC Adv. 1 (2011) 1716.
[32] U. Hauser, V. Oestreich, H.D. Rohrweck, Z. Phys. 280 (1977) 17. A280 (1977) 125; 1978, A284 (1978) 9.
[33] J.A. Güida, O.E. Piro, P.J. Aymonino, Solid State Commun. 57 (1986) 175.
[34] D.B. Soria, J.I. Amalvy, O.E. Piro, E.E. Castellano, P.J. Aymonino, J. Chem. Crystallogr. 26 (1996) 325. and references therein.
[35] J.A. Güida, O.E. Piro, P.J. Aymonino, Solid State Commun. 66 (1988) 1007.
[36] L.A. Gentil, J.A. Olabe, E.J. Baran, P.J. Aymonino, J. Therm. Anal. 7 (1975) 279.
[37] H. Inoue, S. Narino, N. Yoshioka, E. Fluck, Z. Naturforsch. 55b (2000) 685.
[38] R. Robinette, R.L. Collins, J. Coord. Chem. 4 (1974) 65. and references therein.
[39] K. Nakamoto, Infrared and Raman Spectra of Inorganic and Coordination Compounds, sixth ed., Wiley, 2009.
[40] G.J. Kubas, Chem. Rev. 107 (2007) 4152.
[41] A. Hamaed, M. Trudeau, D.M. Antonelli, J. Am. Chem. Soc. 130 (2008) 6992.
[42] T.K.A. Hoang, M.I. Webb, H.V. Mai, A. Hamaed, C.J. Walsby, M. Trudeau, D.M. Antonelli, J. Am. Chem. Soc. 132 (2010) 11792.
[43] C. Prestipino, L. Regli, J.G. Vitillo, F. Bonino, A. Damin, C. Lamberti, A. Zecchina, P.L. Solari, K.O. Kongshaug, S. Bordiga, Chem. Mater. 18 (2006) 1337.
[44] D.R. Lide (Ed.), CRC Handbook of Chemistry and Physics, 84th ed., CRC Press, FL, USA, 2004.
[45] R.D. Shannon, Acta Crystallogr. 32A (1976) 751.